Journal of Stress Analysis
Vol. 9, No. 1, 2025, 109-117
Bu-Ali Sina University

ORIGINAL RESEARCH PAPER

Effect of Finite Size on the Thermal Conductivity of MgO: A Molecular Dynamics Study

Alireza Lotfalinezhad[a], **Ali Rajabpour**[b,*], **Seyed Abbas Sadat Sakak**[b]

[a] Department of Mechanical Engineering, K. N. Toosi University of Technology, Tehran, Iran.
[b] Department of Mechanical Engineering, Imam Khomeini International University, Qazvin, Iran.

Article info

Article history:
Received 19 April 2025
Received in revised form
23 June 2025
Accepted 28 June 2025

Keywords:
Thermal conductivity
MD
Magnesium oxide
Nanostructures

Abstract

Magnesium oxide (MgO) nanostructures have garnered considerable interest due to their distinctive characteristics, including a high surface-to-volume ratio, enhanced chemical reactivity, and exceptional thermal and mechanical stability. In this study, the thermal conductivity of MgO nanostructures was systematically investigated across various simulation configurations by using molecular dynamics study (MD) and Born–Mayer–Huggins potential. Two sets of simulations were conducted: one involving nanostructures of varying lengths with a fixed cross-sectional width, and another involving structures of constant length with variable cross-sectional widths. The results demonstrate a clear positive correlation between crystal length and thermal conductivity at room temperature, with conductivity values approaching approximately $27 W \cdot m^{-1} \cdot K^{-1}$ for sufficiently long structures. In contrast, variations in cross-sectional width were found to have negligible impact on thermal conductivity (ranging from 11.9 to $12.5 W \cdot m^{-1} \cdot K^{-1}$), indicating that length plays a more dominant role in heat transport within MgO nanostructures. The data presented in this study may also exhibit up to a 5% deviation from the actual values.

Nomenclature

K	Thermal conductivity	q	Energy rate
T	Temperature	x	Length
A	Cross-sectional area of the MgO nanostructure		

1. Introduction

The thermal conductivity of materials is critically important for their application at high temperatures. However, accurate measurement of thermal conductivity remains challenging [1]. Magnesium oxide (MgO), a component of Earth's mantle, exhibits an NaCl-type crystal structure. Researchers have shown significant interest in MgO and have employed various methods to investigate its physical properties under high temperature and high-pressure conditions. Notably, the thermal conductivity of MgO decreases from $30 W \cdot m^{-1} \cdot K^{-1}$ at room temperature to $8 W \cdot m^{-1} \cdot K^{-1}$ at elevated temperatures [2]. Magnesium oxide (MgO) possesses both thermal and electrical insulating proper-

*Corresponding author: A. Rajabpour (Associate Professor)
E-mail address: a.rajabpour@gmail.com
10.22084/jrstan.2025.31739.1272
ISSN: 2588-2597

ties, characterized by its cubic crystal structure. Interatomic interactions at high temperatures, in conjunction with particle position alterations and phonon vibrations, have been demonstrated using molecular dynamics (MD) simulations [3, 4]. As electronic devices become more compact and powerful, managing internal heat becomes vital. Therefore, materials that combine electrical insulation with high thermal conductivity, especially inorganic/polymer composites are increasingly explored for efficient heat dissipation in microelectronics and energy systems [5-8]. Magnesium (Mg) alloys have emerged as leading sustainable engineering materials in the 21st century, owing to their rich natural abundance, low density, excellent thermal and electrical conductivities, and strong electromagnetic shielding capabilities [9-11]. To enhance their mechanical strength, alloying elements are commonly introduced into the α-Mg matrix. However, while this approach improves structural performance, it often comes at the cost of reduced thermal conductivity, a trade-off that poses challenges for applications requiring efficient heat dissipation [9,12-14].

One-dimensional (1D) nano-structures, including nanowires, nanorods, nanobelts, nanoribbons, nanoneedles, and nanotubes, have garnered significant interest owing to their distinctive and intriguing properties, along with their promising technological applications [15]. 1D nano-structures are increasingly recognized as essential components of nanoscale photonic devices, including light-emitting diodes, photodiodes, lasers, active waveguides, and integrated electro-optic modulators. This is primarily due to their superior luminescence efficiency [16,17]. Among the metal oxides examined, magnesium oxide (MgO) has garnered particular significant attention. Characterized as a typical wide band gap insulator with a band gap of 7.8eV, MgO exhibits appealing electronic and optical properties. Its low heat capacity and high melting point further enhance its suitability for insulation applications [18]. Magnesium oxide (MgO) nanostructures serve as protective layers for dielectrics in alternating current (AC) circuits. Their application enhances discharge characteristics and extends the service life of panels. This improvement is attributed to their anti-sputtering properties, high transmittance, and favorable secondary electron emission coefficient [19].

In work done by Cha et al., researchers developed a lightweight, self-supporting MgO framework composed of smooth-surfaced, thermally conductive MgO spheres using the finite element method. The authors emphasized that the interconnected MgO spheres formed continuous heat-transfer channels, minimizing interfacial thermal resistance and enhancing overall composite performance. The results demonstrated a substantial increase in thermal conductivity for the 3D-MgO/epoxy composite up to $1.56\mathrm{W{\cdot}m^{-1}{\cdot}K^{-1}}$, which is more than three times higher than that of the randomly dispersed MgO composite. These simulations confirmed that the 3D filler architecture facilitated more efficient heat transfer across the composite. The results concluded that this strategy offers a scalable and effective route for designing high-performance thermal interface materials, especially for electronics and energy systems requiring efficient thermal management [20].

Liu et al. developed humidity-stable submicron magnesium oxide (MgO) particles to enhance thermal conductivity in polymer composites while maintaining performance under moist conditions. By modifying the surface of MgO particles to resist water absorption, they achieved uniform dispersion and strong interfacial bonding within the matrix, resulting in efficient heat transfer pathways. Experimental measurements showed thermal conductivity values reaching up to $2.1\mathrm{W{\cdot}m^{-1}{\cdot}K^{-1}}$, significantly higher than those of conventional MgO composites. Finite element simulations confirmed that the improved filler architecture and moisture resistance contributed to consistent and elevated thermal performance, making these composites suitable for demanding thermal management applications [21].

Luo, Stevens, and Taylor measured the thermal diffusivity of magnesium oxide reinforced with silicon carbide (SiC) particles using the laser flash technique over a temperature range of 200–1000°C. Thermal conductivity was then calculated by combining the diffusivity data with measured density and specific heat. The results showed that adding SiC significantly enhanced the thermal conductivity of the MgO matrix, especially at elevated temperatures. The authors also developed a modified Eshelby inclusion model to account for porosity and particle interactions in the composite, providing a better fit to the experimental data. This work highlights the potential of MgO/SiC composites for high-temperature thermal management applications where both conductivity and structural stability are critical [22].

Rudajevová and Lukáč conducted experimental measurements on several Mg-based alloys, including pure Mg, AZ91, QE22, and Mg-Sc, using the laser flash method to determine thermal diffusivity across a temperature range up to 300°C. Specific heat and density data were used to calculate thermal conductivity. The results showed that thermal conductivity increased with temperature for all tested alloys, with pure Mg exhibiting the highest values. The presence of alloying elements such as aluminum, zinc, and rare earths influenced phonon scattering and microstructure, leading to variations in thermal transport behavior. These findings are relevant for applications in lightweight structural components and thermal management systems where Mg alloys are exposed to elevated temperatures [23].

This research aims to explore the thermal conduc-

tivity of magnesium oxide (MgO) nanostructures by utilizing molecular dynamics (MD) simulations. The study focuses on varying the length and cross-sectional areas of the nanostructures to assess their impact on thermal conductivity. To obtain the thermal conductivity values, hot and cold bathes are established at both ends of the MgO nano-structure.

2. Simulation Details

To investigate the thermal transport behavior of MgO at the nanoscale, a computational framework illustrated in Fig. 1 was adopted for both modeling and simulation purposes. The figure presents a representative nano-structure with a square cross-sectional geometry, precisely defined by a width of 3.3nm and a longitudinal extension of 24nm. This configuration was selected to capture the essential characteristics of MgO when confined to nanoscale dimensions, where surface effects, phonon scattering, and quantum confinement begin to significantly influence thermal properties. The structure serves as a prototype for exploring MgO's potential in advanced applications such as nanoelectronics, thermal interface materials, and energy storage systems, where efficient heat dissipation is critical.

The central aim of this study is to systematically analyze how thermal conductivity varies with changes in the nano-structure's length and to quantify the influence of surface area modifications on heat transport efficiency. By simulating multiple configurations with varying aspect ratios and boundary conditions, the research seeks to uncover scaling laws and interfacial phenomena that govern thermal conduction in MgO nanostructures. Detailed dimensional parameters used in the simulations, including discrete values for length and width, are comprehensively listed in Table 1 and Table 2, providing a basis for comparative analysis and reproducibility.

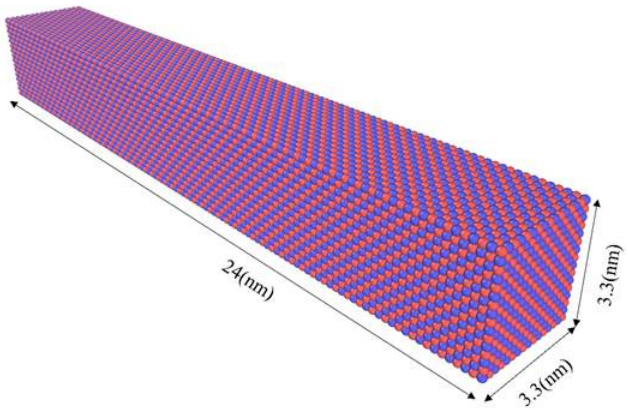

Fig. 1. Atomistic sample model of a MgO nanostructure with a rectangular prism geometry, measuring 24nm in total length and 3.3nm in both width and height. The alternating red and blue spheres represent Mg^{2+} and O^{2-} ions arranged in a crystalline lattice.

Fig. 2 presents a schematic representation of the MgO unit cell lattice, illustrating its fundamental ionic architecture. Within this structure, magnesium ions (Mg^{2+}) are positioned at regular intervals, each paired with oxygen ions (O^{2-}) to form a highly ordered cubic lattice. The $+2$ and -2 charges on the respective ions generate strong electrostatic attractions, which are central to the compound's structural integrity and thermal stability. These ionic bonds not only define the crystalline arrangement but also underpin MgO's notable physical properties, including its high melting point, electrical insulation capability, and relevance in high-temperature and geophysical applications.

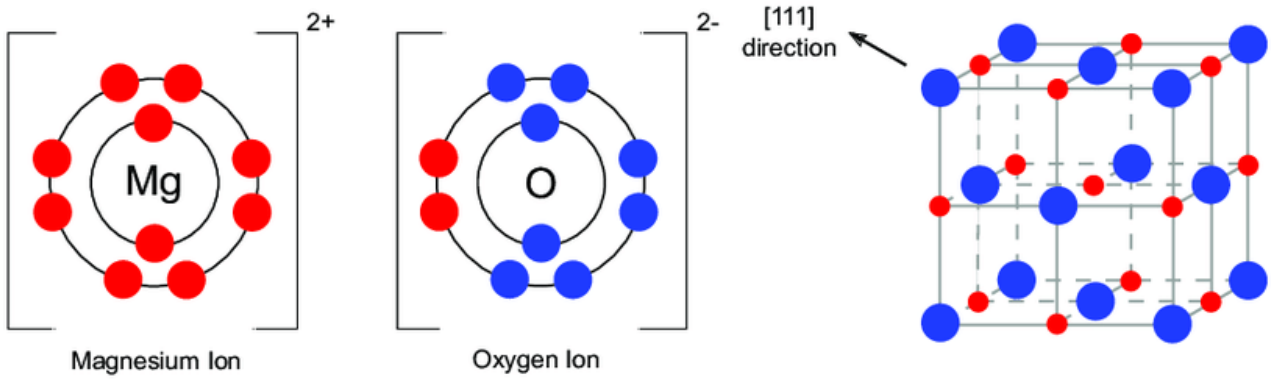

Fig. 2. Schematic representation of the unit cell of MgO, illustrating the cubic crystal lattice composed of Mg^{2+} and O^{2-} ions. The positively charged magnesium ions and negatively charged oxide ions are arranged in a face-centered cubic (FCC) structure.

To accurately determine the thermal conductivity of the MgO nanostructure, a non-equilibrium molecular dynamics (NEMD) approach was employed. As illustrated in Fig. 3, the simulation domain was divided into three distinct regions: a central measurement zone flanked by two thermal reservoirs. The right-hand side of the structure was designated as the hot bath, maintained at a temperature of 320K (47°C), while the left-hand side served as the cold bath, held at 280K (7°C). These thermal regions, each with a fixed length of 1nm, were implemented using Nose–Hoover thermostats to impose and sustain the temperature gradient necessary for heat flux generation. The central region of the nanostructure, situated between the thermal baths, was used to compute the steady-state thermal conductivity based on Fourier's law. To minimize the influence of artificial reflections and periodic boundary artifacts, both ends of the nanostructure were extended by 5nm and kept fixed throughout the simulation. This buffer zone ensured that the imposed temperature gradient remained stable and that phonon transport was not disrupted by boundary effects.

All simulations were conducted using the Large-scale Atomic/Molecular Massively Parallel Simulator (LAMMPS), a widely adopted molecular dynamics engine for nanoscale thermal transport studies. A time step of 1 femtosecond was chosen to resolve atomic vibrations with high temporal fidelity. The system was equilibrated using the canonical ensemble (NVT), with a temperature relaxation time of 100 picoseconds applied to both thermal reservoirs. This allowed the system to reach a quasi-steady state before thermal conductivity measurements were taken. The simulation protocol involved monitoring the energy exchange between the thermal baths and the central region over time, enabling the calculation of heat flux. Combined with the imposed temperature gradient, these data were used to extract the effective thermal conductivity of the MgO nanostructure. The Born–Mayer–Huggins (BMH) potential was employed to simulate the ionic structure of magnesium oxide. This potential effectively captures Coulombic interactions, short-range repulsion between ions, and long-range electrostatic forces. A cutoff radius of 10 Å was used, and periodic boundary conditions were applied in all three spatial directions. The methodology provides insight into how nanoscale confinement, surface effects, and boundary conditions influence thermal transport in ionic solids like MgO.

To analyze the spatial distribution of heat transfer within the central region of the MgO nanostructure depicted in Fig. 3, this region was discretized into a series of uniformly sized segments along the longitudinal axis. The local temperature in each segment was computed to construct a detailed temperature profile, enabling the identification of steady-state gradients and potential non-linearities in thermal transport. This segmentation approach facilitates a more accurate application of Fourier's law for calculating thermal conductivity, particularly in nanoscale systems where temperature fluctuations and boundary effects can be significant.

Table 1 outlines the total lengths of the MgO nanostructures simulated in this study. The central region length, isolated from the thermal reservoirs, defines the domain over which thermal conductivity was evaluated. This region excludes the fixed and thermostatic zones to ensure that the calculated values reflect intrinsic material behavior rather than boundary-induced artifacts.

Table 2 summarizes the range of cross-sectional widths used in the simulations. Each width corresponds to a square cross-section, and thus the cross-sectional area was determined by squaring the width value. This parameter plays a critical role in defining the heat flux and, consequently, the effective thermal conductivity. By varying both the length and width of the nanostructures, the study systematically explores the influence of geometric scaling on thermal transport in MgO at the nanoscale.

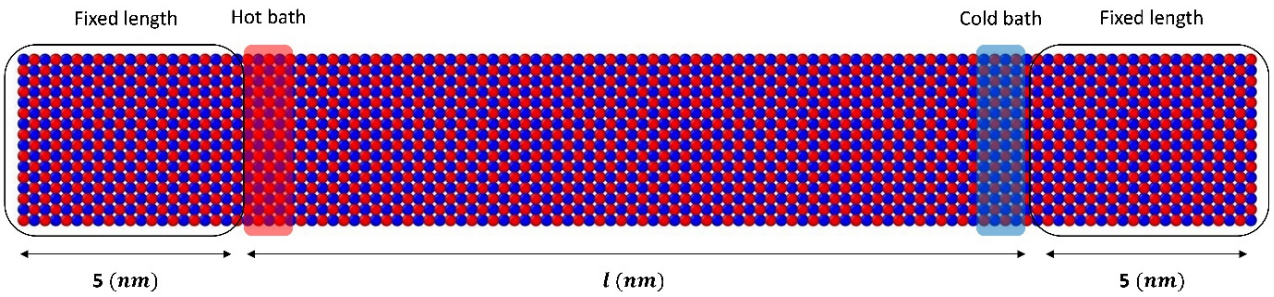

Fig. 3. Side view of the MgO nanostructure used for thermal conductivity analysis, with dimensions of 24nm in total length and 3.3nm in width. The simulation setup includes two thermal reservoirs: a hot bath at 320K (red) and a cold bath at 280K (blue), each extending 1 nm after fixed length zones. The central region, where temperature gradients are measured, is used to evaluate steady-state heat transport under imposed thermal conditions.

Table 1
Geometric configurations used for thermal conductivity calculations in MgO nanostructures. All simulations were conducted with a fixed cross-sectional width of 3.3nm, while the central length of the nanostructure was varied to assess its influence on thermal transport properties.

Width (nm)	Central length (nm)	Cross-sectional (nm^2)	Number of atoms
3.3	14	10.89	29696
3.3	28	10.89	55150
3.3	40	10.89	61440
3.3	50	10.89	86016
3.3	70	10.89	102400
3.3	80	10.89	110592

Table 2
Cross-sectional width configurations used for thermal conductivity calculations in MgO nanostructures. All simulations were conducted at a fixed central length of 14nm, while the width was varied to assess its influence on thermal transport behavior.

Width (nm)	Central length	Cross-sectional area (nm^2)	Number of atoms
3.3	14	10.89	29696
6.5	14	42.25	118784
10	14	100	267264

3. Results and Discussion

According to the findings reported in [2], the thermal conductivity of the magnesium oxide (MgO) nanostructure at room temperature is measured to be approximately 30W·m^{-1}·K^{-1}, indicating its strong potential for nanoscale heat dissipation applications. To quantify this property, the study employs Fourier's law of heat conduction, which relates the heat flux to the temperature gradient across a material. This relationship is mathematically expressed in Eq. (1), where the thermal conductivity K is derived from the ratio of the heat transfer rate to the product of the temperature difference and the cross-sectional area, normalized by the length of the conduction path.

In the molecular dynamics (MD) simulations conducted, a controlled temperature gradient is imposed across the MgO nanostructure, and the resulting heat flux is monitored over time. By evaluating the steady-state energy exchange between the hot and cold regions, the thermal conductivity is calculated in units of watts per meter per Kelvin (W·m^{-1}·K^{-1}).

$$\mathrm{k} = -\frac{\mathrm{q}}{\mathrm{AdT/dx}} \tag{1}$$

Fig. 4 illustrates the temperature gradient established across the MgO nanostructure, extending from the hot bath to the cold bath. The total length of the structure in this configuration is 24nm, and the figure clearly demonstrates a linear temperature profile, indicative of steady-state heat conduction. This linearity confirms the validity of the simulation setup and supports the application of Fourier's law for thermal conductivity calculations. To quantify the temperature distribution along the central region of the nanostructure, the domain was discretized into uniform segments, each measuring 0.5nm in length. The temperature within each segment was computed by averaging atomic velocities over the course of the simulation, specifically at the 3-nanosecond mark, once thermal equilibrium had been reached.

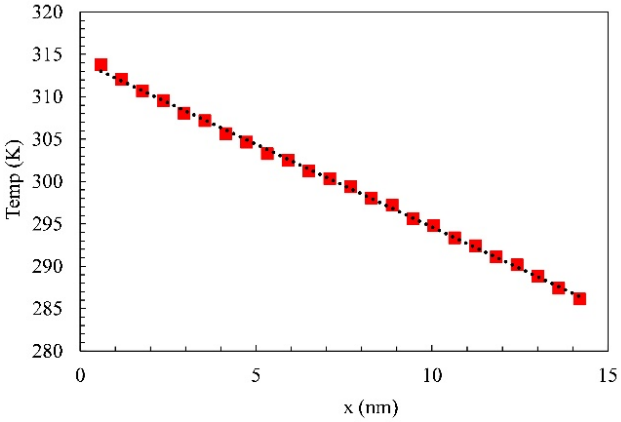

Fig. 4. Temperature distribution along the length of the MgO nanostructure under steady-state conditions. The linear gradient, spanning from 320K to 280K across a 14nm central length, reflects uniform heat conduction. The slope of the given fit is -1.9547 and quality fit of 0.99%.

Based on the temperature profile illustrated in Fig. 4, the spatial temperature gradient $\frac{\mathrm{dT}}{\mathrm{dx}}$ across the central region of the MgO nanostructure (according to Fig. 3) was calculated to be 1.97K nm^{-1}. This gradient is a critical parameter for determining the thermal conductivity using Eq. (1), derived from Fourier's law of heat conduction. Figure 5 presents the temporal evolution of energy exchange during the simulation, plotted as a function of time. The energy-time plot captures the cumulative energy transferred between the thermal reservoirs and the central region, providing insight into the steady-state heat flux established during the simulation.

To quantify the heat flux, the energy values associated with the hot and cold baths were extracted by subtracting the time variable from the cumulative energy data. This yielded opposing energy distributions: q_h = 57.45kcal/mol.ps for the hot bath and q_c = 57.43kcal/mol.ps for the cold bath. The near-symmetry of these values confirms the stability and accuracy of the simulation, indicating minimal energy loss and consistent thermal exchange. These values are subsequently used to compute the net heat flux q in SI units, which, when combined with the temperature gradient $\frac{dT}{dx}$, enables the calculation of the thermal conductivity K of the MgO nanostructure in units of W·m^{-1}·K^{-1}.

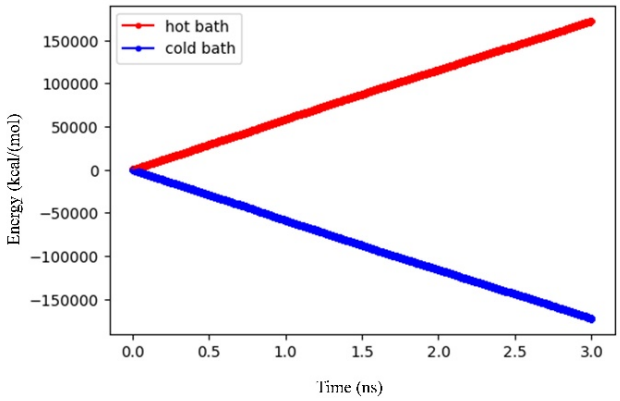

Fig. 5. Accumulated energy transfer from the hot bath to the cold bath over the simulation duration of 3ns. The linear and symmetric trends confirm a steady-state heat flux, with final energy values of $q_h = +57.45$kcal/mol.ps and $q_c = -57.43$kcal/mol.ps, indicating consistent thermal exchange and minimal energy loss across the MgO nanostructure.

To convert the given units of (kcal/mol.ps) into the SI units, Eq. (2) is used as well.

$$q_{SI} = q_{h,c} \times \frac{4184\text{J}}{1\text{kcal}} \times \frac{1}{6.022 \times 10^{23}\text{mol}} \times \frac{1\text{fs}}{10^{-15}\text{s}} \qquad (2)$$

Using Eqs. (1) and (2), the thermal conductivity $K$of the magnesium oxide (MgO) nanostructure was calculated for each configuration listed in "Table 1" and "Table 2". The required parameters namely the temperature gradient $\frac{dT}{dx}$, the cross-sectional area A, and the net heat flux q were obtained from molecular dynamics simulations. The cross-sectional area was determined by squaring the width values provided in Table 2, while the heat flux was derived from the energy exchange between the hot and cold thermal reservoirs. These inputs enabled precise computation of K in units of watts per meter per Kelvin ($\text{W}\cdot\text{m}^{-1}\cdot\text{K}^{-1}$) for each nanostructure geometry.

Fig. 6 presents the calculated thermal conductivity values as a function of nanostructure length, based on the configurations detailed in Table 1. Due to intrinsic computational uncertainties in molecular dynamics simulations, the reported values may exhibit up to 5% variation. The data reveal a clear trend: as the length of the MgO nanostructure increases, the computed thermal conductivity values gradually approach an asymptotic limit. This convergence suggests that beyond a certain length scale, the influence of boundary scattering and finite-size effects diminishes, allowing the material to exhibit bulk-like thermal transport behavior. The observed trend underscores the importance of geometric scaling in nanoscale heat conduction. Shorter structures are more susceptible to phonon-boundary interactions, which suppress thermal conductivity, whereas longer structures allow for more complete phonon propagation and energy transfer.

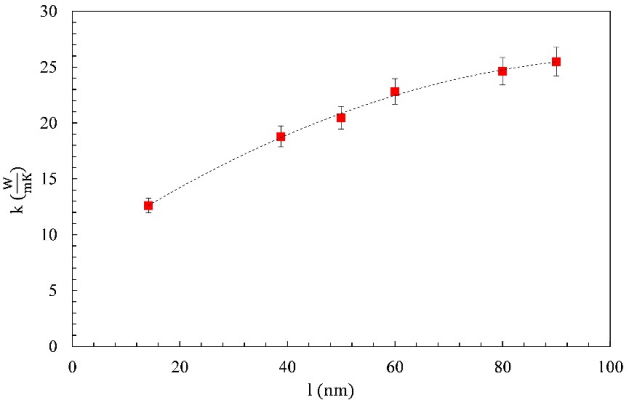

Fig. 6. Thermal conductivity of MgO nanostructures as a function of length, based on molecular dynamics simulations. The data show an increasing trend with length, converging toward an asymptotic value of approximately $27\text{W}\cdot\text{m}^{-1}\cdot\text{K}^{-1}$. calculated values have 5% uncertainty.

To estimate the thermal conductivity of magnesium oxide (MgO) nanostructures at infinite length where boundary scattering effects are negligible, a two-step extrapolation method was employed. The first step involves plotting the inverse thermal conductivity (1/K) against the inverse length (1/L) of the nanostructure, as shown in Fig. 7. This approach is grounded in the kinetic theory of phonon transport, where finite-size effects cause deviations from bulk thermal behavior. The linearity of the plot in Fig. 7 confirms that the relationship between 1/K and 1/L can be approximated by a first-order regression model. From the linear fit, the intercept on the vertical axis represents the inverse of the thermal conductivity in the limit of infinite length ($L \to \infty$). This extrapolated value accounts for intrinsic phonon transport mechanisms, excluding boundary-induced scattering. Based on the obtained model, the slope of the fitted line is 0.1983 with an intercept of 0.036. Furthermore, the quality of fit for the plot in Fig. 7 is 0.857.

In the second step, the data from Fig. 7 are used to reconstruct the direct relationship between thermal conductivity $K$and nanostructure length L, as illustrated in Figure 8. This plot provides a visual representation of how thermal conductivity increases with length and asymptotically approaches the bulk value. The convergence behavior observed in Fig. 8 reinforces the validity of the extrapolation method and highlights the importance of length-dependent scaling in nanoscale thermal transport.

The results illustrated in Figure 8 reinforce the trend observed in Fig. 6, demonstrating that the thermal conductivity of MgO nanostructures increases with length and gradually converges toward an asymptotic limit. The extrapolated asymptotic thermal conductivity value determined in this study is $27\text{W}\cdot\text{m}^{-1}\cdot\text{K}^{-1}$, representing the effective conductivity in the limit of infinite length.

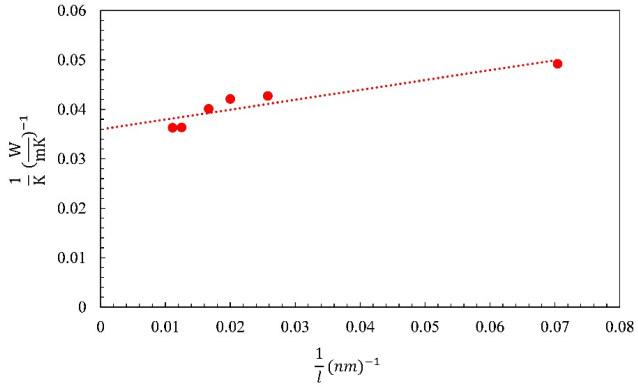

Fig. 7. Plot of inverse thermal conductivity $\left(\frac{1}{K}\right)$ versus inverse length $\left(\frac{1}{L}\right)$ for MgO nanostructures. The linear relationship enables extrapolation of thermal conductivity in the infinite-length limit, where boundary scattering effects are minimized. The fitted line exhibits a slope of 0.1983 and an intercept of 0.036, with a R^2 of 0.857.

This value shows strong agreement with the experimentally reported bulk thermal conductivity of MgO, which is approximately $30 W \cdot m^{-1} \cdot K^{-1}$, as cited in reference [2]. The close alignment between simulation and experimental data validates the modeling approach and confirms the reliability of the extrapolation method used.

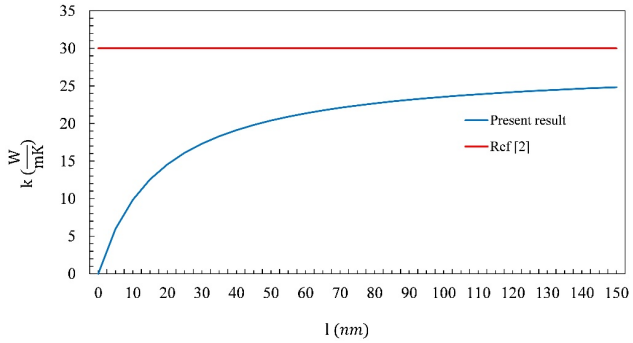

Fig. 8. Thermal conductivity of magnesium oxide nanostructures as a function of length. The graph shows that thermal conductivity increases with length and asymptotically approaches $27 W \cdot m^{-1} \cdot K^{-1}$ for sufficiently long structures.

It also highlights the potential of molecular dynamics simulations to accurately capture nanoscale thermal transport phenomena and predict bulk-like behavior under appropriate geometric conditions. These findings underscore the importance of length-dependent scaling in thermal conductivity analysis and provide a foundation for optimizing MgO-based materials in applications where heat dissipation is critical, such as nanoelectronics, thermal interface layers, and high-temperature insulators.

Fig. 9 illustrates the relationship between thermal conductivity and the cross-sectional width of MgO nanostructures, based on molecular dynamics simulations. The analysis encompasses three distinct width configurations 3.3nm, 6.5nm, and 10nm, each corresponding to square cross-sectional geometries. The results indicate that variations in cross-sectional width within this range exert minimal influence on the calculated thermal conductivity values. This negligible dependence suggests that, for MgO nanostructures of sufficient length, thermal transport is predominantly governed by longitudinal phonon propagation rather than transverse dimensional constraints. The insensitivity of thermal conductivity to cross-sectional width can be attributed to the relatively short phonon mean free paths in the transverse direction and the dominance of boundary scattering effects at the nanoscale. These findings imply that, beyond a certain threshold, increasing the cross-sectional area does not significantly enhance heat conduction, making width a less critical parameter in thermal design optimization for MgO-based nano-devices.

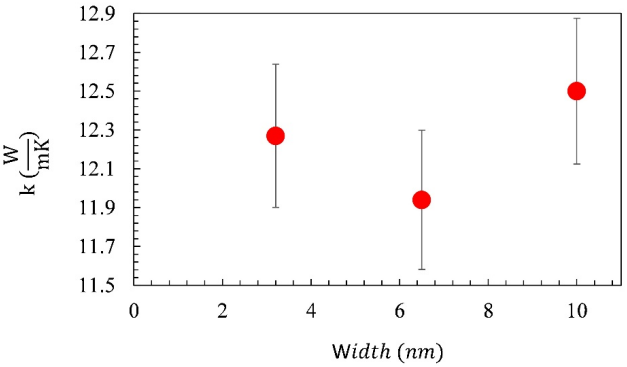

Fig. 9. Thermal conductivity measurements of MgO nanostructures with varying cross-sectional widths (3.3nm, 6.5nm, and 10nm) at l=14nm length with deviation of 5%. The results indicate that thermal conductivity remains nearly constant across the tested width range, suggesting that transverse dimensions have negligible influence on heat transport under the given simulation conditions.

Moreover, the simulation results exhibit strong agreement with experimentally reported trends, reinforcing the validity of the computational framework and the reliability of the interatomic potentials used. This alignment underscores the predictive capability of molecular dynamics in capturing nanoscale thermal phenomena and supports the use of MgO as a stable and efficient thermal conductor in applications where dimensional constraints are present.

4. Conclusions

In this study, the thermal transport properties of MgO nanostructures were systematically investigated using molecular dynamics (MD) simulations. The simulation framework was designed to explore the influence of geometric parameters, specifically length and cross-sectional width, on the thermal conductivity of MgO

at the nanoscale. Two sets of configurations were considered: one with varying total lengths of 24, 38, 50, 60, 80, and 90nm at a fixed width of 3.3nm, and another with varying widths of 3.3, 6.5, and 10nm at a constant length of 24nm.

The results reveal a pronounced dependence of thermal conductivity on the length of the nanostructure. As the length increases, the thermal conductivity exhibits an asymptotic rise, ultimately converging toward a saturation value of approximately $27 W \cdot m^{-1} \cdot K^{-1}$. This asymptotic behavior is consistent with the suppression of boundary scattering effects in longer structures, allowing for more complete phonon propagation. Notably, the simulated saturation value aligns closely with experimentally reported bulk thermal conductivity values for MgO, which are typically around $30 W \cdot m^{-1} \cdot K^{-1}$, thereby validating the accuracy of the MD approach and the interatomic potentials employed.

In contrast, the influence of cross-sectional width on thermal conductivity was found to be negligible within the tested range. For widths of 3.3, 6.5, and 10nm, the thermal conductivity values remained largely invariant, suggesting that transverse confinement plays a minimal role in heat transport for MgO nanostructures of this scale. This observation underscores the dominance of longitudinal phonon transport and supports the conclusion that thermal conductivity in MgO nanostructures is primarily governed by length-dependent scaling. The findings of this study, along with prior research in the field, suggest that introducing vacancy defects into the ionic surface structure of magnesium oxide enables a more realistic representation of its nonstructural behavior. This approach enhances the accuracy of simulations and theoretical models. Furthermore, integrating MgO nanostructures with other ionic compounds such as NaCl may offer synergistic effects, potentially improving material performance or enabling novel functionalities. These findings provide valuable insights into the design of MgO-based materials for thermal management applications, particularly in nanoelectronics and high-temperature environments where efficient heat dissipation is critical.

References

[1] T. Seetawan, G. Wong-Ud-Dee, C. Thanachayanont, A. Vittaya. Molecular dynamics simulation of strontium titanate, Chin. Phys. Lett., 27 (2010) 0260501.

[2] J. A. Slifka, D. K. Filla, J. M. Phelps Thermal conductivity of magnesium oxide from absolute, steady-state measurements, J. Res. Natl. Inst. Stand. Technol., (1998) 357.

[3] X. Sun, Q. Chen, Y. Chu, C. Wang. Properties of MgO at high pressure: shell-model molecular dynamics simulation, Physica B, (2005) 187-188.

[4] B. G. Dick, A. W. Overhauser. Theory of the dielectric constants of alkali halide crystals, Phys. Rev., 112(1) (1958) 90-103.

[5] E. S. Lee, S. M. Lee, D. J. Shanefield, W. R. Cannon. Enhanced thermal conductivity of polymer matrix composite via high solids loading of aluminum nitride in epoxy resin, J. Am. Ceram. Soc., 91(4) (2008) 1169-1174.

[6] K. Sato, H. Horibe, T. Shirai, Y. Hotta, H. Nakano, H. Nagai, K. Mitsuishi, K. Watari. Thermally conductive composite films of hexagonal boron nitride and polyimide with affinity-enhanced interfaces, J. Mater. Chem., 20(14) (2010) 2749-2752.

[7] B. Deepanraj, N. Senthilkumar, G. Hariharan, T. Tamizharasan, T. T. Bezabih. Numerical modelling, simulation, and analysis of the end-milling process using DEFORM-3D with experimental validation, Adv. Mater. Sci. Eng., (2022), Article ID 5692298.

[8] M. Tanimoto, T. Yamagata, K. Miyata, S. Ando. Anisotropic thermal diffusivity of hexagonal boron nitride-filled polyimide films: effects of filler particle size, aggregation, orientation, and polymer chain rigidity, ACS Appl. Mater. Interfaces, 5(11) (2013) 4374-4382.

[9] S. Li, X. Yang, J. Hou, W. Du. A review on thermal conductivity of magnesium and its alloys, J. Magnes. Alloys, 8 (2020) 78-90.

[10] J. Bai, Y. Yang, C. Wen, J. Chen, G. Zhou, B. Jiang, X. Peng, F. Pan. Applications of magnesium alloys for aerospace: a review, J. Magnes. Alloys, 11 (2023) 3609-3619.

[11] W. Zhang, M. Ma, J. Yuan, et al.. Microstructure and thermophysical properties of Mg−2Zn−xCu alloys, Trans. Nonferrous Met. Soc. China, 30 (2020) 1803-1815.

[12] G. Li, J. Zhang, R. Wu, et al.. Development of high mechanical properties and moderate thermal conductivity cast Mg alloy with multiple RE via heat treatment, J. Mater. Sci. Technol., 34 (2018) 1076-1084.

[13] V. Bazhenov, A. Koltygin, M. Sung, et al., Development of Mg–Zn–Y–Zr casting magnesium alloy with high thermal conductivity, J. Magnes. Alloys, 9 (2021) 1567-1577.

[14] J. Rong, J. Zhu, W. Xiao, X. Zhao, and C. Ma. A high pressure die cast magnesium alloy with superior thermal conductivity and high strength, Intermetallics, (2021) 139, Article ID 107350.

[15] G. Hodes. Advanced Materials, 27 (2007) 639-657.

[16] S. Noda, N. Yamamoto, M. Imada, H. Kobayashi, M. Okano. Alignment and stacking of semiconductor photonic bandgaps by wafer-fusion, Lightwave Technol., (1999) 1948-1955.

[17] W. Qingqing, X. Gang, H. Gaorong. Solvothermal synthesis and characterization of uniform CdS nanowires in high yield, Solid State Chem., 178 (2005) 2680-2685.

[18] M. C. Wu, J. S. Corneille, C. A. Estrada, J. W. He, D. W. Goodman. Synthesis and characterization of ultra-thin MgO films on Mo (100), Chem. Phys. Lett., 182 (1991) 472-478.

[19] Y. W. Choi, J. Kim. Reactive sputtering of magnesium oxide thin film for plasma display panel applications, Thin Solid Films, (2004) 295-299.

[20] H.-A. Cha, S.-J. Ha, M.-G. Jo, Y. K. Moon, J.-J. Choi, B.-D. Hahn, C.-W. Ahn, and D. K. Kim. Three-dimensional MgO filler networking composites with significantly enhanced thermal conductivity, Adv. Compos. Hybrid Mater., 7(1) (2024) 1-11.

[21] J.-Y. Jeon, Y.-R. Kwak, D.-G. Shin, H.-A. Cha, J.-J. Choi, B.-D. Hahn, C.-W. Ahn, Y. K. Moon. Humidity-stable submicron magnesium oxide particles for high-performance thermally conductive composites, J. Mater. Chem. A, 11(38) (2023) 20096-20104.

[22] J. Luo, R. Stevens, and R. Taylor. Thermal diffusivity/conductivity of magnesium oxide/silicon carbide composites, J. Am. Ceram. Soc., 80(4) (1997) 1004-1008.

[23] A. Rudajevová, P. Lukáč. Thermal diffusivity and thermal conductivity of Mg alloys, Acta Univ. Carol. Math. Phys., 41(1) (2000) 3 -36.